Effects and mechanism of Rictor interference in podocyte injury induced by high glucose

YAN ZENG, CHANGBIN XIONG, YINXIANG CHEN, CHUNYUN YANG and QIUYUE LI

Department of Nephrology, The First Affiliated Hospital of Nanchang University, Nanchang, Jiangxi 330006, P.R. China

Received August 14, 2023; Accepted July 7, 2023

DOI: 10.3892/etm.2023.12172

Abstract. Rapamycin-insensitive companion of mTOR (Rictor) is a critical effector of mTOR protein complex 2 (mTORC2). The aim of the present study was to investigate the effect of Rictor in the mTORC2 signaling pathway in high glucose (HG)-induced diabetic podocyte injury by silencing the expression of Rictor. In the present study, mouse podocytes were treated with glucose (150 mM) and mannitol (200 mM), the *Rictor* gene was silenced using small interfering RNA (siRNA). Apoptosis was detected by flow cytometry, whereas podocyte cytoskeletal protein expression was detected by western blotting (WB) and immunofluorescence staining. The results demonstrated that, compared with that in the control group, the podocyte apoptotic rate was significantly increased in the mannitol group (negative group) and the groups that were treated with glucose (model groups). The podocyte apoptotic rate in the model + *Rictor* siRNA group was significantly decreased compared with that in the negative, model and the model glucose + siRNA negative control (NC) groups. WB indicated that the protein expression levels of podocalyxin and synaptopodin were reduced in the model and model + siRNA NC groups compared with those in the normal control and negative groups. Additionally, the protein expression levels of α-smooth muscle actin (α-SMA) and P-AKT/AKT were increased in the model and model + siRNA NC groups compared with the those in control and negative groups. Compared with those the model and model + siRNA NC groups, the protein expression levels of podocalyxin and synaptopodin were increased, whilst those of the α-SMA and P-AKT/AKT proteins were decreased, in the model + Rictor siRNA group. Results from immunofluorescence analysis were basically consistent with those of WB. Therefore, results of the present study suggest that silencing of the *Rictor* gene may reduce the damage to podocytes induced by HG, such that the Rictor/mTORC2 signaling pathway may be involved in the remodeling of podocyte actin cytoskeletal in diabetes.

Correspondence to: Dr Qiuyue Li, Department of Nephrology, The First Affiliated Hospital of Nanchang University, 17 Yongwaizheng Street, Nanchang, Jiangxi 330006, P.R. China
E-mail: lqy0259@163.com

Key words: podocyte injury, rapamycin-insensitive companion of mTOR, high glucose, diabetic nephropathy

Introduction

Even during the early stages, diabetic kidney disease (DKD) can cause damage to the function and structure of podocytes (1-3). A series of changes occur in the kidney after diabetic podocyte injury, including epithelial-to-mesenchymal transition, and hypertrophy, detachment and apoptosis of podocytes (4-6). Previous studies have revealed that mTOR blockers such as rapamycin can upregulate podocyte autophagy (7), reduce podocyte damage and serve a role in maintaining podocyte cell cycle and protein synthesis (8). In DKD podocyte injury, mTOR can induce changes in numerous podocyte marker proteins, such as up-regulation of α-smooth muscle actin (α-SMA), down-regulation of Ezrin, zona occludens 1 (ZO-1) and CD2 associated protein (CD2AP). The mTOR signaling pathway exists in two forms, mTOR protein complex (mTORC)1 and mTORC2. mTORCl is composed of mTOR, proline-rich Akt substrate 40 kDa, regulatory-associated protein of the mTOR complex 1 (Raptor) and mLST8. By contrast, mTORC2 includes mTOR, proline-rich 5, mLST8, rapamycin-insensitive companion of mTOR (Rictor) and MAPK-associated protein 1 (9,10). Unlike other subunits, Rictor is a protein found specifically as a component of mTORC2 (11).

A previous study reported that a podocyte-specific *Rictor*/mTOR-deficient mouse exhibited no overt clinical, histological or ultrastructural abnormalities (12). Only transient albuminuria was observed in *Rictor*/mTOR-deficient mice treated with bovine serum protein (BSA), which quickly returned to normal. This suggests that mTORC2 can serve a role in regulating and reorganizing the foot process form of podocytes when podocytes are stimulated (10,13). In a number of patients with kidney or heart transplants respectively, long-term use of the mTOR blocker rapamycin can lead to proteinuria (13). Furthermore, prolonged rapamycin therapy can reduce Rictor expression and Rictor/mTOR formation, resulting in reduced AKT phosphorylation, in addition to reducing the expression of transient receptor potential cation channel subfamily C member 6 (TRPC6) and the cytoskeletal regulatory protein non-catalytic region of tyrosine kinase adaptor protein 1 (14). Consequently, podocyte movement and adhesive capacity are reduced. However, the Rictor/mTOR signaling pathway has no effect on podocyte

TRPC6 expression (14,15), suggesting that the Raptor/mTOR signaling pathway may be involved in the remodeling of the podocyte actin cytoskeleton in DKD. At present, there is no specific mTORC2 blocker. In a previous study, the dual blocker of mTORC1 and mTORC2 KU0063974 and rapamycin a blocker of mTORC1, were used to observe their effects on podocyte injury induced by high glucose (HG). It was revealed that KU0063974 could effectively preserve Ezrin and α-SMA protein expression in podocytes, while rapamycin had no effect (16). Therefore, for the present study it was hypothesized that the mTORC2 signaling pathway may be involved in HG-induced podocyte injury, by possibly interfering with the remodeling of the podocyte actin cytoskeleton. The present study investigated the effect of the Rictor/mTORC2 signaling pathway on HG-induced podocyte injury by silencing the Rictor expression using small-interfering RNA (siRNA).

Materials and methods

Materials. Mouse MPC5 podocytes (cat. no. iCell-m081, iCell Bioscience, Inc.), DAPI (cat. no. KGA215-50; Nanjing KeyGen Biotech Co., Ltd.), TRIzon reagent (cat. no. CW0580S; CoWin Biosciences), Ultra pure RNA extraction kit (cat. no. CW0581M; CoWin Biosciences), HiScript II Q RT SuperMix for qPCR (+gDNA wiper; cat. no. R223-01; Vazyme Biotech Co., Ltd.), ChamQ Universal SYBR qPCR Master Mix (cat. no. Q711-02; Vazyme Biotech Co., Ltd.), 50X TAE buffer (cat. no. T1060; Beijing Solarbio Science & Technology Co., Ltd.), 6X DNA Loading Buffer (cat. no. GH101-01; TransGen Biotech Co., Ltd.), 50 bp DNA Ladder (cat. no. MD108; Tiangen Biotech Co., Ltd.); Gsafe Red plus nucleic acid dye (cat. no. GK20002; GlpBio Technology), agarose (cat. no. 75510-019; Invitrogen; Thermo Fisher Scientific, Inc.), primary antibody for α-SMA (1:1,000; cat. no. ab124964; Abcam), primary antibody for podocalyxin (1:1,000; cat. no. ab154305; Abcam), primary antibody for synaptopodin (1:1,000; cat. no. ab224491; Abcam), primary antibody for phosphorylated (p-)AKT (1:1,000; cat. no. AF0016; Affinity Biosciences.), primary antibody for AKT (1:1,000; cat. no. bs-6951R; BIOSS), The secondary antibody used was HRP-conjugated goat anti-Rabbit IgG (H+L; 1:2,000; cat. no. ZB-2301; Beijing ZSGB Biotechnology) and HRP-conjugated goat anti-Mouse IgG (H+L; 1:2,000; cat. no. ZB-2305; Beijing ZSGB Biotechnology) RIPA cell lysis buffer (cat. no. C1053; Beijing Pulilai Gene Technology Co., Ltd.), BCA protein quantification kit (BCA Protein Assay kit; cat. no. E-BC-K318-M; Elabscience Biotechnology, Inc.), Pre-stained protein ladder(cat. no. 26617; Thermo Fisher Scientific, Inc.), PVDF film (cat. no. IPVH00010; MilliporeSigma), skimmed milk powder (cat. no. P1622; Beijing Pulilai Gene Technology Co., Ltd.), BSA (cat. no. A8020; Beijing Solarbio Science & Technology Co., Ltd.), SuperSignal® West Pico Chemiluminescent Substrate (cat. no. RJ239676; Thermo Fisher Scientific, Inc.) and Annexin V-FITC/PI Apoptosis kit (cat. no. AP101-100-kit; Hangzhou Lianke Biotechnology Co., Ltd.).

Methods. MPC5 cells were cultured in DMEM medium (Gibco, Thermo Fisher Scientific, Inc.) supplemented with 10% fetal bovine serum (FBS, cat. no. E600001-0500; BBI Life Sciences Corporation), 1,000 U/l penicillin, 1 mg/l streptomycin (cat. no. 15140148, Gibco, Thermo Fisher Scientific, Inc.) at 37˚C in a 5% CO_2 and 95% air humidified incubator. The aforementioned culture conditions were used for all subsequent experiments unless otherwise specified. After the cells were attached to the wall, mannitol and glucose (0, 25, 50, 100, 150 or 200 mM) were added. After treatment for 24 h, the CCK8 assay was performed to evaluate cell viability. Finally, glucose at 150 mM and mannitol at 200 mM was selected for use in subsequent experiments.

The mouse podocytes were divided into the following five groups: Normal group (control group), mannitol group (200 nM, negative group), glucose group (150 nM, model group), glucose + siRNA negative control (NC) group (model + siRNA NC group) and glucose + *Rictor* siRNA group (model + siRNA group). All groups were treated with mannitol or glucose for 24 h at 37˚C.

CCK-8 assay. The cells were seeded at a density of $5x10^3$ cells/well in a 96-well plate. After the cells were treated, 10 μl CCK8 reagent (cat. no. KGA317; Jiangsu Kaiji Biotechnology Co., Ltd) was added to each well and incubated at 37˚C for 2 h. The absorption value of each well was quantified at 450 nm.

Silencing of Rictor using siRNA-1. Mouse podocytes were treated with glucose, and Cell Counting Kit-8 (CCK-8) assays were used to select the most suitable treatment concentration.

Rictor expression was detected by reverse transcription-quantitative PCR (RT-qPCR). The mouse *Rictor* (NM_030168.3) sequence was obtained from the National Center for Biotechnology Information GenBank (https://www.ncbi.nlm.nih.gov/genbank) (Table I). siRNA (General Biology (Anhui) Co., Ltd.) targeting the *Rictor* gene was then transfected into mouse podocytes. Opti-MEM (125 μl; cat. no. 31985-062; Gibco, Thermo Fisher Scientific, Inc.) was added to two tubes. Subsequently, 5 μl Lipofectamine® 3000 (cat. no. L300015, Invitrogen) was added to one tube, whereas 12.5 μl siRNA was added to the other tube (the siRNA dry powder was dissolved in diethyl pyrocarbonate-treated water; 3 nmol/125 μl). They were then individually incubated at room temperature for 5 min. The contents of the two tubes were then mixed together and the solution was incubated at room temperature for 15 min. This mixed solution was added into a well of a six-well plate with a density of $2x10^5$ cells/well, before the cells were incubated at 37˚C. At 4 h after transfection, 1 ml DMEM with 20% serum was added into each well of the six-well plate. A sample used to verify the success of transfection was obtained 48 h later. RT-qPCR and western blotting (WB) were used to confirm the silencing efficiency. Subsequence experiments were performed 48 h after transfection.

RT-qPCR. Cells were cultured in a petri dish of DMEM medium supplemented with 10% FBS (cat. no. E600001-0500; BBI Life Sciences Corporation), 1,000 U/l penicillin, 1 mg/l streptomycin, at 37˚C and 5% CO_2 before the cell culture medium was removed. Subsequently, 1 ml TRIzon reagent was added to each dish according to the number of cells ($1x10^5$-$1x10^6$ cells/1 ml Trizol) and incubated on ice for 5 min. The cell lysates was transferred into a 1.5 ml tube and 0.2 ml chloroform was added. The content was mixed

Table I. Sequence of the interfering agents and controls.

Name		Sequence 5'-3'
Rictor-siRNA-1	Forward	CAGCAAACUUGUAAAGAAUTT
	Reverse	AUUCUUUACAAGUUUGCUGTT
Rictor-siRNA-2	Forward	GGCCAGACCUCAUGGACAATT
	Reverse	UUGUCCAUGAGGUCUGGCCTT
Rictor-siRNA-3	Forward	CUUAGAAGAUCUCGUGAAATT
	Reverse	UUUCACGAGAUCUUCUAAGTT
siRNA NC	Forward	UUCUCCGAACGUGUCACGUTT
	Reverse	ACGUGACACGUUCGGAGAATT

Rictor, rapamycin-insensitive companion of mTOR; siRNA, small interfering RNA; NC, negative control.

Table II. Information of the primers used.

Primer	Sequence (5'-3')	Product length, bp	Annealing temperature,˚C
Rictor F	ACTGAGCTGTTACTGGGTGTTA	129	58
Rictor R	CTCGTGACACTTGGTGGAAAC		
β-actin F	AGGGAAATCGTGCGTGAC	192	58
β-actin R	CATACCCAAGAAGGAAGGCT		

Rictor, rapamycin-insensitive companion of mTOR; F, forward; R, reverse.

completely and centrifuged at 14,000 x g for 15 min at 4˚C. The upper transparent layer was transferred to a new tube and an equal volume of ethyl alcohol was added. mRNA was then extracted using an Ultra pure RNA extraction kit (cat. no. CW0581M; CoWin Biosciences) according to the manufacturer's instructions. The concentration and integrity of the mRNA were determined using an ultraviolet-visible spectrophotometer [optical density (OD)260/OD280]. cDNA was obtained using an mRNA reverse transcription kit (HiScript II Q RT SuperMix for qPCR with gDNA wiper; cat. no. R223-01; Vazyme Biotech Co., Ltd.). First, gDNA wiper Mix was added into mRNA and incubated at 42˚C for 2 min. Then, HiScript II qRT SuperMix II was added into the product and reacted at 50˚C for 15 min and 85˚C for 5 sec. Fluorescence qPCR was performed using a fluorescence PCR instrument. The reaction system used was as follows: 10 μl 2X SYBR Green PCR Master Mix (ChamQ Universal SYBR qPCR Master Mix, cat. no. Q711-02; Vazyme Biotech Co., Ltd.), 1 μl cDNA, 0.4 μl forward primer, 0.4 μl reverse primer and 8.2 μl RNase-free dH_2O. The reaction steps used were as follows: Initial denaturation at 95˚C for 10 min; followed by 40 cycles of denaturation at 95˚C for 10 sec, annealing at 58˚C for 30 sec and extension at 72˚C for 30 sec. β-actin was used as an internal reference and the relative expression levels of the Rictor mRNA were determined using the $2^{-\Delta\Delta Cq}$ method (17). The primers used are presented in Table II.

WB. Podocytes were incubated with 100 μl cell lysis buffer and placed on ice for 20 min. Cell lysates were extracted scraped and centrifuged at 14,000 x g. for 10 min. The supernatant was then collected and the protein concentration was quantified using a BCA protein assay. Protein samples (20 μg/lane) were denatured and run on a 10% gel for SDS-PAGE for 1.5 h, before being transferred onto PVDF membranes with constant current at 300 mA for 1.5 h. Then the membranes were blocked using 3% skimmed dried milk (cat. no. P1622; Beijing Pulilai Gene Technology Co., Ltd.) in TBST (0.1% Tween 20) for 1 h at room temperature. The PVDF membranes were then incubated with primary antibody overnight at 4˚C, followed by incubation with a secondary antibody for 2 h at room temperature. The membrane was then washed and saturated with ECL (cat. no. RJ239676; Thermo Fisher Scientific, Inc.), before being exposed using an ultra-high sensitivity chemiluminescence imaging system for development.

The primary antibodies used for the present study were as follows: Rabbit anti-α-SMA (1:1,000; cat. no. ab124964; Abcam), rabbit anti-podocalyxin (1:1,000; cat. no. ab154305; Abcam), rabbit anti-synaptopodin (1:1,000; cat. no. ab224491; Abcam), rabbit anti-p-AKT (1:1,000; cat. no. AF0016; Affinity Biosciences) and rabbit anti-AKT (1:1,000; cat. no. bs-6951R; BIOSS). The secondary antibody used was HRP-conjugated goat anti-Rabbit IgG (H+L; 1:2,000; cat. no. ZB-2301; Beijing ZSGB Biotechnology) and HRP-conjugated goat anti-Mouse IgG (H+L; 1:2,000; cat. no. ZB-2305; Beijing ZSGB Biotechnology). GAPDH (1:1,000; cat. no. ab8245; Abcam) was used as an internal control for normalization. GraphPad version 7.0 (Dotmatics) was used to draw and generate graphs. Image-Pro Plus software 6.0 (Media Cybernetics, Inc.) was used for grayscale value analysis.

Flow cytometry apoptosis detection. Annexin V-FITC/PI Apoptosis Kit (cat. no. AP101-100-kit; Multisciences (Lianke) Biotech Co., Ltd.) was used to detect apoptotic cells according to the manufacturer's instructions. Cells (1-3x10^6) were collected, centrifuged with 1 ml PBS at 800 x g for 3 min at room temperature, washed twice and diluted in 5X binding buffer to 1X binding buffer with distilled water. Cells (~1x10^6) were suspended in 300 μl pre-cooled 1X binding buffer, before 5 μl annexin V-FITC and 10 μl PI from the kit were added to the tubes. The solutions were gently mixed and incubated at room temperature in the dark for 10 min. An additional 200 μl pre-cooled 1X binding buffer was added to each tube with gentle mixing. Apoptosis was detected using NovoCyte™ flow cytometry (NovoCyte 2060R; Eisen Bio (Hangzhou) Co., Ltd.). The quantitative data were obtained from the Annexin V-FITC+/PI+ (Q2-2) and Annexin V-FITC+/PI-(Q2-4) cell sum.

Immunofluorescence staining. Mouse podocytes were fixed with 4% paraformaldehyde at 37˚C for 15 min and permeabilized with PBS containing 0.5% Triton X-100 for 5 min at room temperature. Following three washes with PBS for 5 min each, samples were blocked with 5% BSA for 30 min at 37˚C and incubated with the anti-synaptopodin (1:50, cat. no. 21064-1-AP; Proteintech Gorup, Inc.), podocalyxin (1:50, cat. no. bs-1345R, BIOSS); α-SMA (1:50, cat. no. ab5694, Abcam) antibodies at 4˚C overnight. The samples were washed three times in PBS for 5 min each and incubated with a cyanine 3-conjugated secondary antibody (1:100, cat. no. AS007, ABclonal Biotech Co., Ltd.) for 45 min at 37˚C, followed by three washes with PBS. The sample was incubated in the dark with DAPI (cat. no. KGA215-50; Nanjing KeyGen Biotech Co., Ltd.) for nuclear staining for about 5 min at room temperature and sealed with 50% glycerol. Images were captured with a fluorescence microscope.

Statistical analysis. SPSS version 26.0 (IBM Corp.) software and R Programming Language version 4.2.2 (https://cran.r-project.org/) were used for statistical analysis. The Readxl package was used to import data, the Base package was used to perform normality testing (Shapiro-Wilks) and a homogeneity of variance analysis (Bartlett test). All experiments were repeated at least three times, before the quantitative results are presented as the mean ± standard deviation. A Shapiro-Wilk test was conducted to examine the normality of the data, where the samples would be considered to conform to a normal distribution if P>0.05. The Bartlett test was used to test for the homogeneity of variance in the data and P>0.05 would considered to indicate homogeneity of variance among groups. One-way ANOVA was used for multi-group comparisons of data with homogeneity of variance and Tukey's post hoc test was used for multiple comparisons. Welch's ANOVA was used for data with heterogeneity of variance and Tambane's T2 was used for multiple comparisons. All figures were generated using GraphPad Prism 9.3.1 (Dotmatics). P<0.05 was considered to indicate a statistically significant difference.

Results

RT-qPCR was used to confirm successful Rictor knockdown. The results indicated that all three synthetic interference sequences could significantly reduce Rictor mRNA expression (Fig. 1). Rictor-siRNA-1 had the best interference effect, it was selected for use in the subsequent experiments.

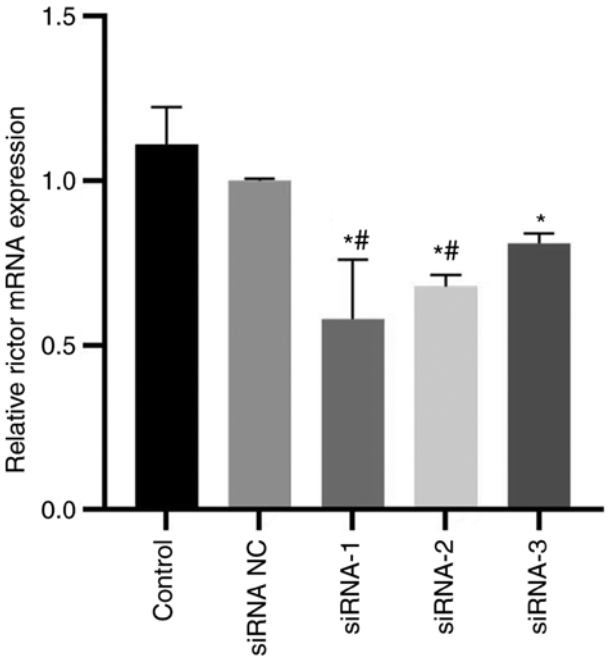

Figure 1. Reverse transcription-quantitative PCR results for Rictor knockdown. All three of siRNA sequences significantly reduced the expression levels of Rictor mRNA. *P<0.05 vs. Control and #P<0.05 vs. siRNA NC. Rictor, rapamycin-insensitive companion of mTOR; siRNA, small interfering RNA; NC, negative control.

Cell activity was detected by cck8. After 24 h of treatment, the cell activity of mannitol group and glucose group decreased significantly. Compared with 0 mm group, the cell activity of the 200 mM mannitol group was significantly decreased, whilst the 100 mM glucose group was significantly decreased. Cell activity in the 150 mM glucose group was comparable with that in the 200 mM mannitol group, 150 mM glucose and 200 mM mannitol were used for the subsequent experiments (Fig. 2).

Apoptosis detection by flow cytometry. Flow cytometry was used to detect the apoptosis of podocytes in each treatment group. The results demonstrated that, compared with that in the control group, the apoptosis rate of podocytes in the negative, model, model + siRNA NC and model + Rictor siRNA groups was significantly increased. Compared with the apoptosis rates of the podocytes in the negative, model and model + siRNA NC groups, the apoptosis rate of podocytes in the model + Rictor siRNA group was significantly decreased (Fig. 3). These results indicated that both HG and mannitol can induce podocyte apoptosis, which was in turn significantly reversed after Rictor knockdown. Therefore, the Rictor/mTOR signaling pathway may be involved in podocyte apoptosis (Fig. 3).

α-SMA, podocalyxin and synaptopodin detection using WB. The expression levels of podocyte cytoskeletal proteins after Rictor knockdown were investigated. Expression of

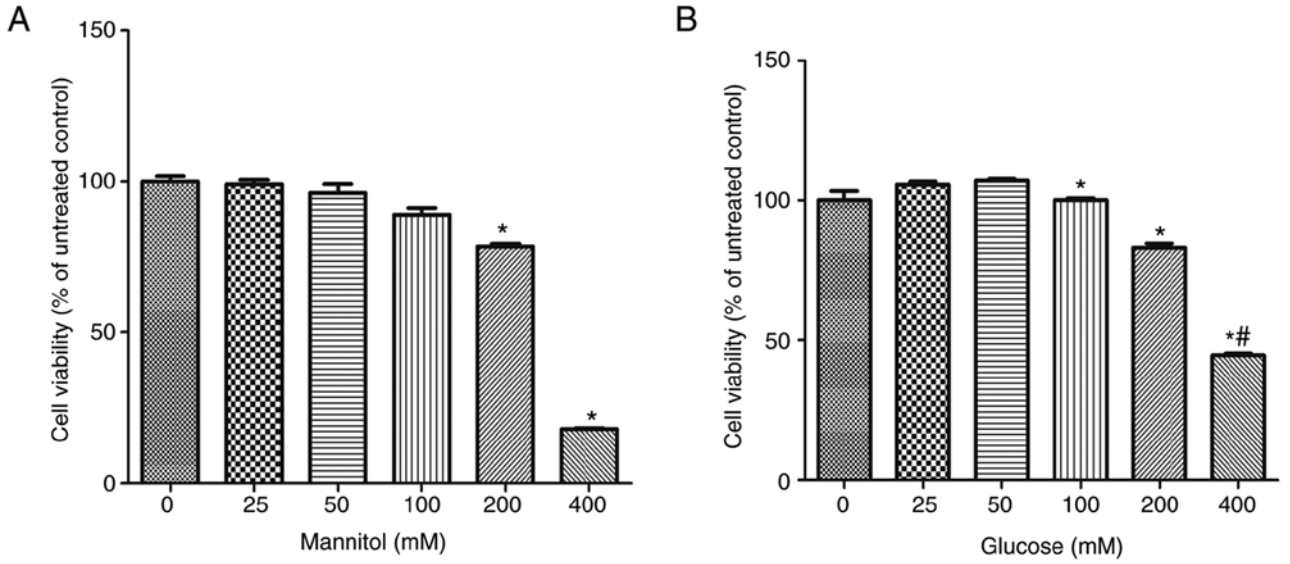

Figure 2. CCK-8 was used to detect cell activity. The cell activity of (A) 200 mM mannitol group and (B) 100 mM glucose group were significantly lower than that of 0 mM group, 150 mM glucose and 200 mM mannitol were used for the subsequent experiments. *P<0.05 vs. 0 mM and #P<0.05 vs. 25 mM.

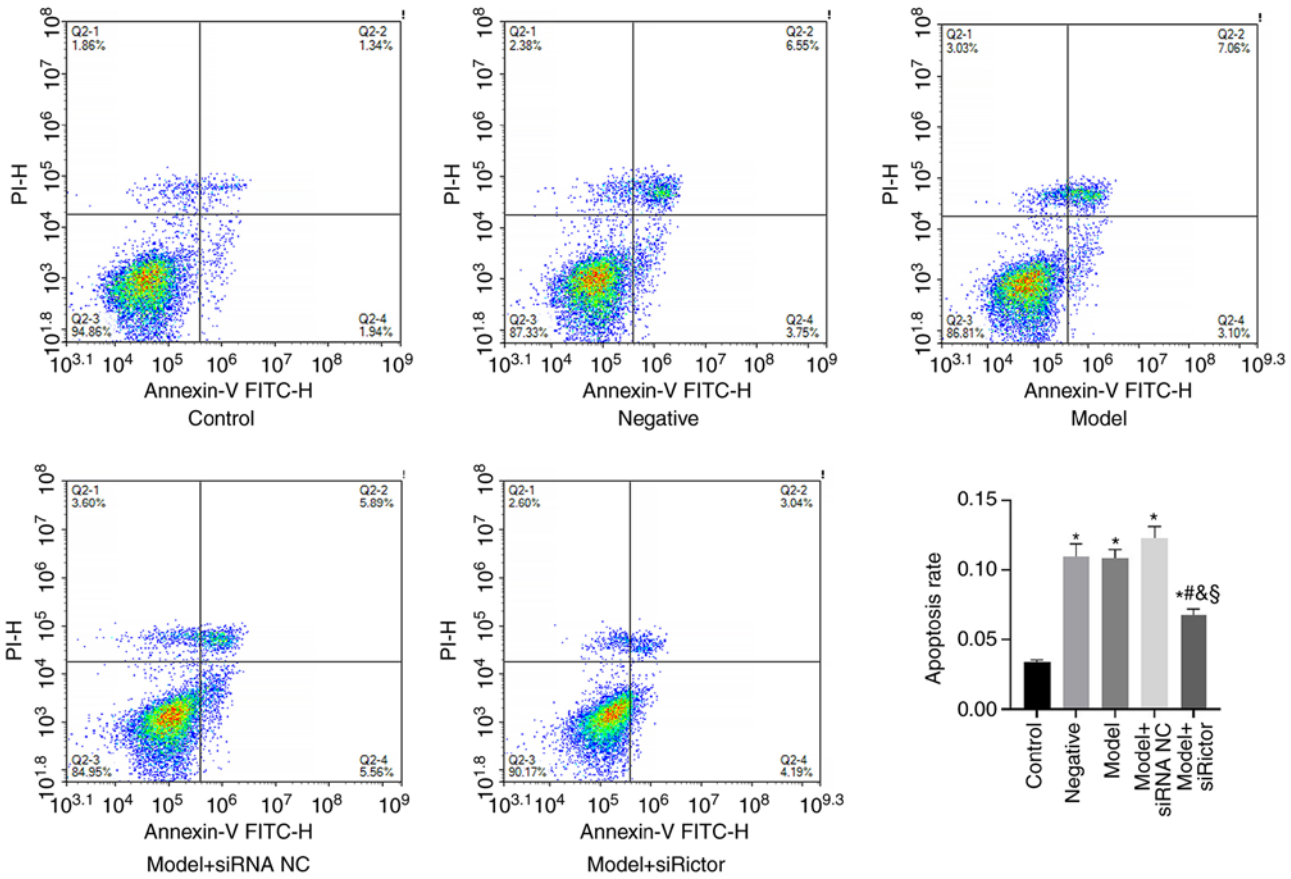

Figure 3. Podocyte apoptosis. The results indicated that both high glucose (model) and high osmotic pressure induced by mannitol (negative) could induce podocyte apoptosis, whereas the apoptosis rate of the podocytes was decreased significantly after Rictor knockdown. This suggest that the Rictor/mTOR signaling pathway is involved in podocyte apoptosis. *P<0.05 vs. Control group, #P<0.05 vs. Negative, §P<0.05 vs. Model and &P<0.05 vs. model + siRNA NC. Rictor, rapamycin-insensitive companion of mTOR; siRNA/si, small interfering RNA; NC, negative control.

the podocyte cytoskeletal proteins α-SMA, podocalyxin and synaptopodin, in addition to AKT and phosphorylated (p)-AKT, were detected by WB. p-AKT is a downstream mediator of the mTORC2 pathway (18), the levels of which can be used to indicate activity of the mTORC2 pathway. The results indicated that compared with those in the control and negative groups, the expression levels of the podocalyxin and synaptopodoin proteins in the model and model + siRNA

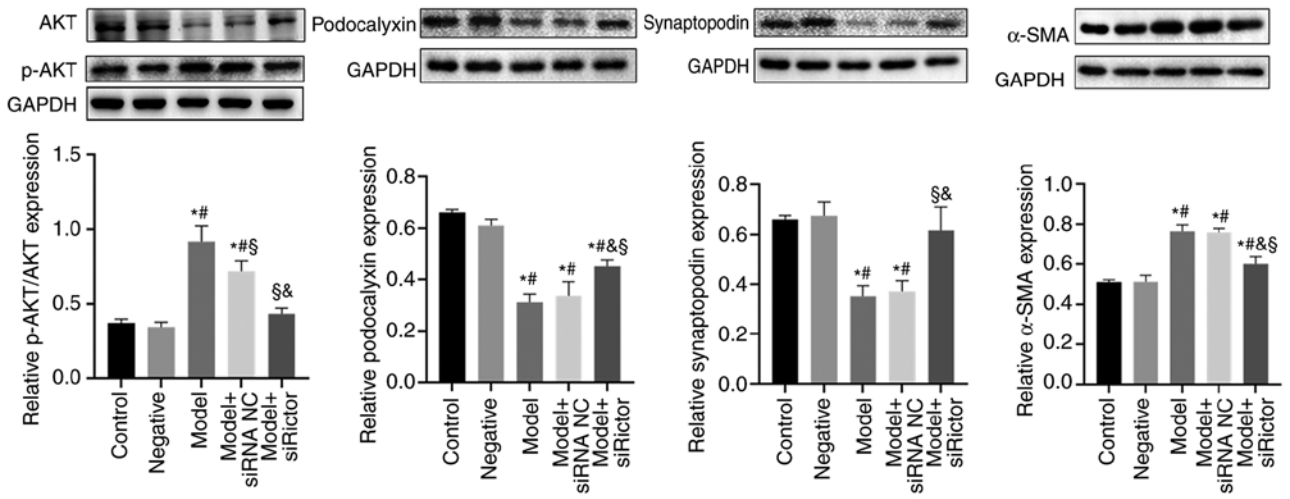

Figure 4. Expression levels of podocyte actin cytoskeleton components. The expression of podocalyxin and synaptopodin in model group and model + siRNA NC group were significantly lower than those in control group and negative group, whilst α-SMA and p-AKT/AKT were significantly increased. Podocalyxin and synaptopodin in model + Rictor siRNA group were significantly higher than those in model group and model + siRNA NC group, whilst α-SMA and p-AKT/AKT were significantly decreased. *P<0.05 vs. Control, #P<0.05 vs. negative, and §P<0.05 vs. Model, &P<0.05 vs. model + siRNA NC group. Rictor, rapamycin-insensitive companion of mTOR; siRNA/si, small interfering RNA; NC, negative control; p-, phosphorylated; α-SMA, α-smooth muscle actin.

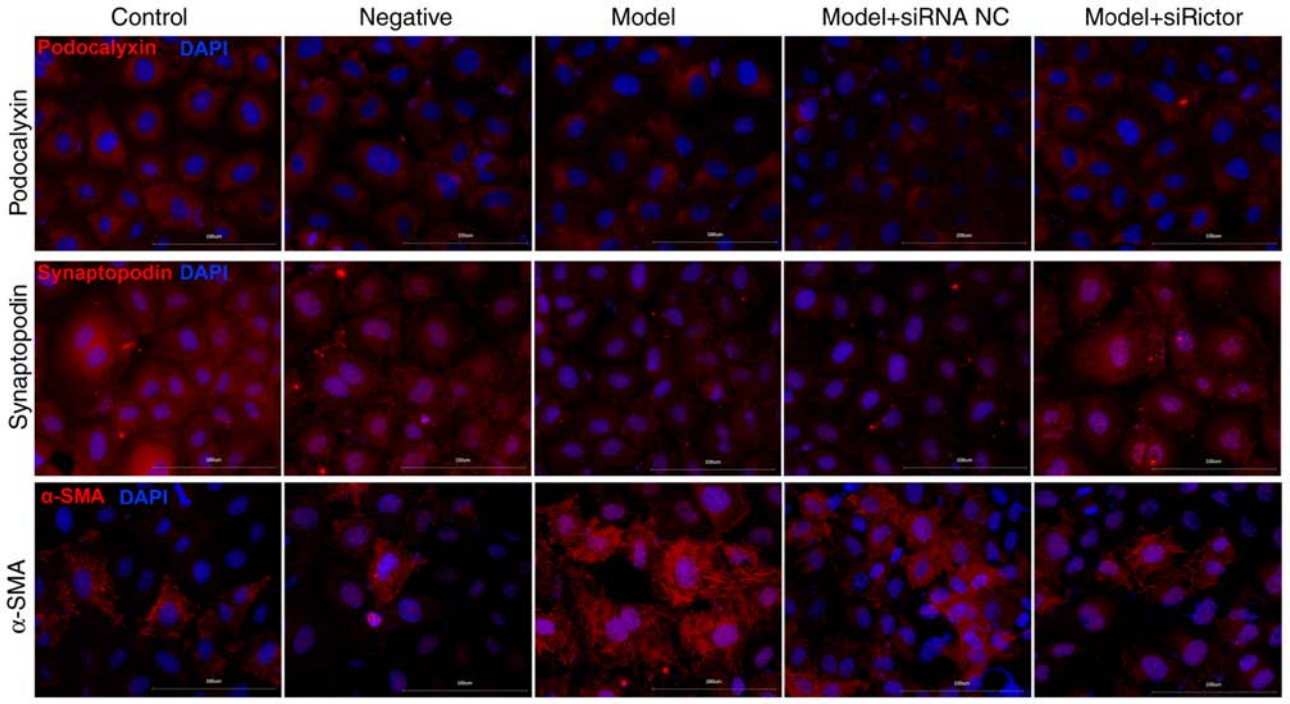

Figure 5. Immunofluorescence staining of podocyte-associated cytoskeletal proteins. Immunofluorescence staining results indicated that podocyte-associated proteins were mainly located on the cell membrane and in the cytoplasm, but not in the nucleus. Target protein in red and DAPI in blue Magnification, x400. Rictor, rapamycin-insensitive companion of mTOR; α-SMA, α-smooth muscle actin; si, small interfering RNA; NC, negative control.

NC groups were decreased, whilst the levels of α-SMA and p-AKT/AKT were significantly increased. After the Rictor expression was knocked down in the podocytes, the expression levels podocalyxin and synaptopodin proteins in the model + Rictor siRNA group were significantly increased compared with those in the model and model + siRNA NC groups, whilst those of α-SMA and p-AKT/AKT were significantly decreased. These results suggest that the Rictor/mTOR signaling pathway was involved in the remodeling of the podocyte actin cytoskeleton (Fig. 4).

Immunofluorescence staining. Immunofluorescence staining results indicated that podocyte-associated proteins were mainly located on the cell membrane and in the cytoplasm (Fig. 5). Compared with those in the control group, the fluorescence densities of podocalyxin and synaptopodin in the model and model + siRNA NC groups were decreased, whilst the fluorescence density of α-SMA was significantly increased. Furthermore, compared with that in the model + siRNA NC group, the fluorescence density of α-SMA in the model + Rictor siRNA group was decreased, whilst that of podocalyxin and

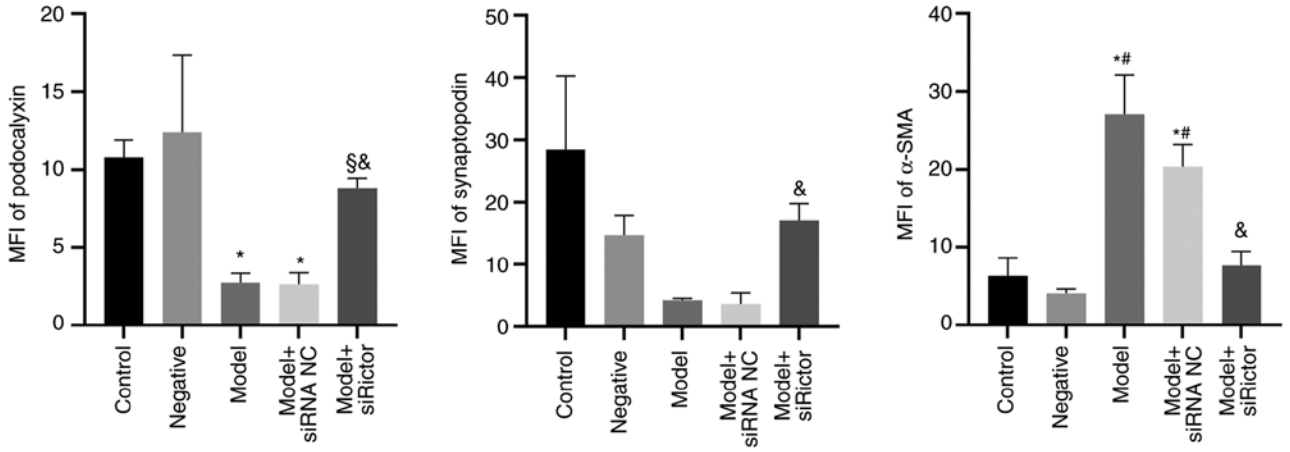

Figure 6. Quantitative analysis of the fluorescence density of podocyte-associated cytoskeletal proteins. The fluorescence density of podocalyxin in model group and model + siRNA NC group was significantly lower than that in the control group, and podocalyxin in model + Rictor siRNA group was significantly higher than that in model group and model + siRNA NC group. The synaptopodin in model + Rictor siRNA group was significantly higher than that in model + siRNA NC group. The fluorescence density of α-SMA in model group and model +siRNA NC group was significantly higher than that in control group and negative group, and α-SMA in model + Rictor siRNA group was significantly lower than that in model +siRNA NC group. *P<0.05 vs. Control, $^{\#}$P<0.05 vs. negative, §P<0.05 vs. Model, $^{\&}$P<0.05 vs. model + siRNA NC groups. Rictor, rapamycin-insensitive companion of mTOR; α-SMA, α-smooth muscle actin; siRNA/si, small interfering RNA; NC, negative control; mean fluorescence intensity (MFI).

synaptopodin were increased. Compared with the model group, podocalyxin expression in the model + *Rictor* siRNA group was also increased. These results suggest that the immunofluorescence analysis results supported those of WB (Figs. 5 and 6).

Discussion

As a part of the glomerular filtration barrier, podocytes are terminally differentiated cells that are arranged outside the glomerular capillaries, and closely related to the occurrence of proteinuria (19,20). Podocytes can promote glomerular development, constitute filtration barrier, regulate glomerular filtration rate, support and maintain capillary loop morphology, combat glomerular internal pressure, synthesize and decompose the glomerular basement membrane, produce vascular endothelial growth factor to regulate endothelial cells, and participate in inflammation and immune response (21). Podocyte injury or loss (including podocyte apoptosis and function loss) are involved in the process of DKD (22). HG can reduce the level of autophagy (23-25), whilst increasing the level of inflammation (26,27) and apoptosis (28). In addition, HG can also lead to an increase in reactive oxygen species, which is also involved in podocyte injury and apoptosis (29,30). HG can also promote the formation of advanced glycation end products, which leads to podocyte apoptosis by activating the p38 MAPK signaling pathway (30).

Podocyte injury is associated with the dysfunction of podocyte-associated proteins (31). Previous studies have revealed that podocyte skeletal destruction can induce podocyte apoptosis (32-34). A previous study revealed that HG reduced Ezrin expression whilst increasing that of α-SMA in podocytes, but the addition of KU0063974 (a dual blocker of mTORC1 and mTORC2) and not rapamycin, reversed these changes (16). This finding suggests that podocyte cytoskeleton-associated proteins may be primarily regulated by the mTORC2 signaling pathway. To investigate this hypothesis, the Rictor expression was knocked down using siRNA, where it was revealed that the podocyte apoptosis decreased significantly after knocking down Rictor. In terms of podocyte cytoskeletal proteins, the protein expression levels of podocalyxin and synaptopodin were decreased whereas those of α-SMA were increased in HG-induced podocytes. Following Rictor knockdown, changes in the expression levels of the aforementioned podocyte cytoskeletal proteins were reversed, suggesting further that these podocyte cytoskeleton-associated proteins were regulated by the Rictor/mTOR signaling pathway. Therefore, these podocyte skeleton-associated proteins may serve a role in podocyte apoptosis. However, although the experiment was repeated numerous times, the *Rictor* protein could not be verified by WB after synthesizing the interference sequence, which is a limitation of the present study.

Previous studies have found that in HG conditions, the expression levels of the podocalyxin (PCX) and nephrin were decreased, whilst the expression of the desmin and α-SMA protein were increased. Furthermore, these changes are associated with the mTOR/PTEN/PI3K/Akt signaling pathway (35,36). Podocalyxin and synaptopodin are apical membrane proteins and cytoskeletal proteins of podocytes, the main roles of which are to maintain the stability of the structure and function of the podocytes (37,38). Decreased expression of these two proteins contributes to podocyte injury (39). Podocalyxin is a key apex membrane protein that is anchored to actin in podocytes, which primarily controls cell adhesion and migration (40,41). In podocyte-associated glomerular diseases, cytoskeletal rearrangements in podocytes and low podocalyxin expression are commonly observed (42-44). As podocalyxin is the predominant glycocalyx protein on podocytes, the anionic charge of this molecule has been considered to function as a charge barrier in glomerular filtration and to serve a charge repulsion role that maintains the space between the podocyte interdigitating foot processes (45). Urinary podocalyxin can be used as a marker for glomerular diseases, such as IgA nephropathy and membranous nephropathy (46).

In addition, podocalyxin is a pathogenic component of focal segmental glomerulosclerosis (FSGS), the complete absence of which leads to congenital nephrotic syndrome (45). Synaptopodin is a linear cytoplasmic protein that is associated with actin filaments (47). Previous studies have revealed that synaptopodin expression varies in different types of disease (48-51). Although synaptopodin expression is typically present in healthy children without kidney disease and patients with minimal change disease, its expression is either decreased or completely absent in patients with FSGS or HIV-associated nephropathy (48,49). α-SMA is an actin isomer that serves a role in fiber formation (52). α-SMA expression is increased in the renal tubular interstitium of DKD mice (53). mTOR is an evolutionarily conserved protein kinase that regulates cellular metabolism, proliferation and apoptosis in eukaryotes (54,55). Blocking the mTOR signaling pathway can protect pancreatic β-cells from apoptosis induced by HG (56). The mTORC2/Akt/NF-κB signaling pathway can mediate the activation of TRPC6 and participates in podocyte apoptosis induced by Adriamycin (15). The mTORC2 signaling pathway can also promote apoptosis induced by reactive oxygen species (57). In addition, activation of mTORC1, which can induce endoplasmic reticulum stress, leads to the apoptosis of podocytes after HG treatment (28). mTORC2 not only regulates the distribution of big-conductance $Ca2^{+}$-activated K^{+} (BK) channels through Akt, but also modulates BK channel protein expression via Serum/glucocorticoid regulated kinase 1 in podocytes, which can regulate cell proliferation, secretion and migration (58). Therefore, these observations indicates that the mTORC2 signaling pathway serves a role in podocyte apoptosis. Results from the present study support this notion, where podocyte apoptosis was induced by interfering with the remodeling of the podocyte actin through the Rictor/mTOR signaling pathway.

The present study mainly focused on the effects of the Rictor/mTOR/Akt signaling pathway on proteins associated with diabetic podocytosis. The Raptor/mTOR/p70S6K signaling pathway was not studied, which is a limitation of the present study. Future studies should examine whether there are downstream crossover factors between these two signaling pathways.

Acknowledgements

Not applicable.

Funding

The present study was supported by the Natural Science Foundation of Jiangxi Province (grant no. S2020ZRMSB0987).

Availability of data and materials

The datasets used and/or analyzed during the current study are available from the corresponding author on reasonable request.

Authors' contributions

YZ and CX performed the experiments. YC and CY performed statistical analysis and drafted the manuscript. QL performed the statistical analysis and designed the present study. All authors read and approved the final version of the manuscript. YZ and QL confirm the authenticity of all the raw data.

Ethics approval and consent to participate

Not applicable.

Patient consent for publication

Not applicable.

Competing interests

The authors declare that they have no competing interests.

References

1. Gnudi L, Coward RJM and Long DA: Diabetic nephropathy: Perspective on novel molecular mechanisms. Trends Endocrinol Metab 27: 820-830, 2016.
2. Tryggvason K, Patrakka J and Wartiovaara J: Hereditary proteinuria syndromes and mechanisms of proteinuria. N Engl J Med 354: 1387-1401, 2006.
3. Siu B, Saha J, Smoyer WE, Sullivan KA and Brosius FC III: Reduction in podocyte density as a pathologic feature in early diabetic nephropathy in rodents: Prevention by lipoic acid treatment. BMC Nephrol 7: 6, 2006.
4. Jo HA, Kim JY, Yang SH, Han SS, Joo KW, Kim YS and Kim DK: The role of local IL6/JAK2/STAT3 signaling in high glucose-induced podocyte hypertrophy. Kidney Res Clin Pract 35: 212-218, 2016.
5. Li S, Sun Z, Zhang Y, Ruan Y, Chen Q, Gong W, Yu J, Xia W, He JC, Huang S, *et al*: COX-2/mPGES-1/PGE2 cascade activation mediates uric acid-induced mesangial cell proliferation. Oncotarget 8: 10185-10198, 2017.
6. Maezawa Y, Takemoto M and Yokote K: Cell biology of diabetic nephropathy: Roles of endothelial cells, tubulointerstitial cells and podocytes. J Diabetes Investig 6: 3-15, 2015.
7. Wu L, Feng Z, Cui S, Hou K, Tang L, Zhou J, Cai G, Xie Y, Hong Q, Fu B and Chen X: Rapamycin upregulates autophagy by inhibiting the mTOR-ULK1 pathway, resulting in reduced podocyte injury. PLoS One 8: e63799, 2013.
8. Kumar S and Tikoo K: Independent role of PP2A and mTORc1 in palmitate induced podocyte death. Biochimie 112: 73-84, 2015.
9. Gaubitz C, Prouteau M, Kusmider B and Loewith R: TORC2 structure and function. Trends Biochem Sci 41: 532-545, 2016.
10. Yasuda M, Tanaka Y, Kume S, Morita Y, Chin-Kanasaki M, Araki H, Isshiki K, Araki S, Koya D, Haneda M, *et al*: Fatty acids are novel nutrient factors to regulate mTORC1 lysosomal localization and apoptosis in podocytes. Biochim Biophys Acta 1842: 1097-1108, 2014.
11. Ballesteros-Álvarez J and Andersen JK: mTORC2: The other mTOR in autophagy regulation. Aging Cell 20: e13431, 2021.
12. Gödel M, Hartleben B, Herbach N, Liu S, Zschiedrich S, Lu S, Debreczeni-Mór A, Lindenmeyer MT, Rastaldi MP, Hartleben G, *et al*: Role of mTOR in podocyte function and diabetic nephropathy in humans and mice. J Clin Invest 121: 2197-2209, 2011.
13. Aliabadi AZ, Pohanka E, Seebacher G, Dunkler D, Kammerstätter D, Wolner E, Grimm M and Zuckermann AO: Development of proteinuria after switch to sirolimus-based immunosuppression in long-term cardiac transplant patients. Am J Transplant 8: 854-861, 2008.
14. Ding F, Zhang X, Li X, Zhang Y, Li B and Ding J: Mammalian target of rapamycin complex 2 signaling pathway regulates transient receptor potential cation channel 6 in podocytes. PLoS One 9: e112972, 2014.
15. Zhang HT, Wang WW, Ren LH, Zhao XX, Wang ZH, Zhuang DL and Bai YN: The mTORC2/Akt/NFκB pathway-mediated activation of TRPC6 participates in adriamycin-induced podocyte apoptosis. Cell Physiol Biochem 40: 1079-1093, 2016.
16. Li Q, Zeng Y, Jiang Q, Wu C and Zhou J: Role of mTOR signaling in the regulation of high glucose-induced podocyte injury. Exp Ther Med 17: 2495-2502, 2019.

17. Livak KJ and Schmittgen TD: Analysis of relative gene expression data using real-time quantitative PCR and the 2(-Delta Delta C(T)) method. Methods 25: 402-408, 2001.
18. Lou JS, Xia YT, Wang HY, Kong XP, Yao P, Dong TTX, Zhou ZY and Tsim KWK: The WT1/MVP-Mediated Stabilization on mTOR/AKT axis enhances the effects of cisplatin in non-small cell lung cancer by a reformulated Yu Ping Feng San Herbal Preparation. Front Pharmacol 9: 853, 2018.
19. Shankland SJ: The podocyte's response to injury: Role in proteinuria and glomerulosclerosis. Kidney Int 69: 2131-2147, 2006.
20. Coward RJ, Foster RR, Patton D, Ni L, Lennon R, Bates DO, Harper SJ, Mathieson PW and Saleem MA: Nephrotic plasma alters slit diaphragm-dependent signaling and translocates nephrin, Podocin, and CD2 associated protein in cultured human podocytes. J Am Soc Nephrol 16: 629-637, 2005.
21. Dalla Vestra M, Masiero A, Roiter AM, Saller A, Crepaldi G and Fioretto P: Is podocyte injury relevant in diabetic nephropathy? Studies in patients with type 2 diabetes. Diabetes 52: 1031-1035, 2003.
22. Zhang C, Hou B, Yu S, Chen Q, Zhang N and Li H: HGF alleviates high glucose-induced injury in podocytes by GSK3β inhibition and autophagy restoration. Biochim Biophys Acta 1863: 2690-2699, 2016.
23. Xu L, Fan Q, Wang X, Li L, Lu X, Yue Y, Cao X, Liu J, Zhao X and Wang L: Ursolic acid improves podocyte injury caused by high glucose. Nephrol Dial Transplant 32: 1285-1293, 2017.
24. Sun J, Li ZP, Zhang RQ and Zhang HM: Repression of miR-217 protects against high glucose-induced podocyte injury and insulin resistance by restoring PTEN-mediated autophagy pathway. Biochem Biophys Res Commun 483: 318-324, 2017.
25. Miaomiao W, Chunhua L, Xiaochen Z, Xiaoniao C, Hongli L and Zhuo Y: Autophagy is involved in regulating VEGF during high-glucose-induced podocyte injury. Mol Biosyst 12: 2202-2212, 2016.
26. Wei M, Li Z, Xiao L and Yang Z: Effects of ROS-relative NF-κB signaling on high glucose-induced TLR4 and MCP-1 expression in podocyte injury. Mol Immunol 68 (2 Pt A): 261-271, 2015.
27. Li J, Wang B, Zhou G, Yan X and Zhang Y: Tetrahydroxy stilbene glucoside alleviates high glucose-induced MPC5 podocytes injury through suppression of NLRP3 inflammasome. Am J Med Sci 355: 588-596, 2018.
28. Lei J, Zhao L, Zhang Y, Wu Y and Liu Y: High glucose-induced podocyte injury involves activation of mammalian target of rapamycin (mTOR)-Induced endoplasmic reticulum (ER) stress. Cell Physiol Biochem 45: 2431-2443, 2018.
29. Song S, Qiu D, Shi Y, Wang S, Zhou X, Chen N, Wei J, Wu M, Wu H and Duan H: Thioredoxin-interacting protein deficiency alleviates phenotypic alterations of podocytes via inhibition of mTOR activation in diabetic nephropathy. J Cell Physiol 234: 16485-16502, 2019.
30. Song S, Qiu D, Wang Y, Wei J, Wu H, Wu M, Wang S, Zhou X, Shi Y and Duan H: TXNIP deficiency mitigates podocyte apoptosis via restraining the activation of mTOR or p38 MAPK signaling in diabetic nephropathy. Exp Cell Res 388: 111862, 2020.
31. McNicholas BA, Eng DG, Lichtnekert J, Rabinowitz PS, Pippin JW and Shankland SJ: Reducing mTOR augments parietal epithelial cell density in a model of acute podocyte depletion and in aged kidneys. Am J Physiol Renal Physiol 311: F626-F639, 2016.
32. Huang Z, Zhang L, Chen Y, Zhang H, Yu C, Zhou F, Zhang Z, Jiang L, Li R, Ma J, *et al*: RhoA deficiency disrupts podocyte cytoskeleton and induces podocyte apoptosis by inhibiting YAP/dendrin signal. BMC Nephrol 17: 66, 2016.
33. Schell C and Huber TB: The evolving complexity of the podocyte cytoskeleton. J Am Soc Nephrol 28: 3166-3174, 2017.
34. Zhang Y, Xu C, Ye Q, Tong L, Jiang H, Zhu X, Huang L, Lin W, Fu H, Wang J, *et al*: Podocyte apoptosis in diabetic nephropathy by BASP1 activation of the p53 pathway via WT1. Acta Physiol (Oxf) 232: e13634, 2021.
35. Loeffler I and Wolf G: Epithelial-to-Mesenchymal transition in diabetic nephropathy: Fact or fiction? Cells 4: 631-652, 2015.
36. Xing L, Liu Q, Fu S, Li S, Yang L, Liu S, Hao J, Yu L and Duan H: PTEN inhibits high glucose-induced phenotypic transition in podocytes. J Cell Biochem 116: 1776-1784, 2015.
37. Ha TS, Nam JA, Seong SB, Saleem MA, Park SJ and Shin JI: Montelukast improves the changes of cytoskeletal and adaptor proteins of human podocytes by interleukin-13. Inflamm Res 66: 793-802, 2017.
38. Woychyshyn B, Papillon J, Guillemette J, Navarro-Betancourt JR and Cybulsky AV: Genetic ablation of SLK exacerbates glomerular injury in adriamycin nephrosis in mice. Am J Physiol Renal Physiol 318: F1377-F1390, 2020.
39. Daehn IS and Duffield JS: The glomerular filtration barrier: A structural target for novel kidney therapies. Nat Rev Drug Discov 20: 770-788, 2021.
40. Fernández D, Horrillo A, Alquezar C, González-Manchón C, Parrilla R and Ayuso MS: Control of cell adhesion and migration by podocalyxin. Implication of Rac1 and Cdc42. Biochem Biophys Res Commun 432: 302-307, 2013.
41. Nielsen JS, Graves ML, Chelliah S, Vogl AW, Roskelley CD and McNagny KM: The CD34-related molecule podocalyxin is a potent inducer of microvillus formation. PLoS One 2: e237, 2007.
42. Oh J, Reiser J and Mundel P: Dynamic (re)organization of the podocyte actin cytoskeleton in the nephrotic syndrome. Pediatr Nephrol 19: 130-137, 2004.
43. Kavoura E, Gakiopoulou H, Paraskevakou H, Marinaki S, Agrogiannis G, Stofas A, Boletis I, Patsouris E and Lazaris AC: Immunohistochemical evaluation of podocalyxin expression in glomerulopathies associated with nephrotic syndrome. Hum Pathol 42: 227-235, 2011.
44. Weinhold B, Sellmeier M, Schaper W, Blume L, Philippens B, Kats E, Bernard U, Galuska SP, Geyer H, Geyer R, *et al*: Deficits in sialylation impair podocyte maturation. J Am Soc Nephrol 23: 1319-1328, 2012.
45. Kang HG, Lee M, Lee KB, Hughes M, Kwon BS, Lee S, McNagny KM, Ahn YH, Ko JM, Ha IS, *et al*: Loss of podocalyxin causes a novel syndromic type of congenital nephrotic syndrome. Exp Mol Med 49: e414, 2017.
46. Imaizumi T, Nakatochi M, Akiyama S, Yamaguchi M, Kurosawa H, Hirayama Y, Katsuno T, Tsuboi N, Hara M and Maruyama S: Urinary podocalyxin as a biomarker to diagnose membranous nephropathy. PLoS One 11: e0163507, 2016.
47. Ha TS, Choi JY, Park HY and Han GD: Changes of podocyte p130Cas in diabetic conditions. J Nephrol 26: 870-876, 2013.
48. Barisoni L, Kriz W, Mundel P and D'Agati V: The dysregulated podocyte phenotype: A novel concept in the pathogenesis of collapsing idiopathic focal segmental glomerulosclerosis and HIV-associated nephropathy. J Am Soc Nephrol 10: 51-61, 1999.
49. Kemeny E, Dürmüller U, Nickeleit V, Gudat F and Mihatsch MJ: Distribution of podocyte protein (44 KD) in different types of glomerular diseases. Virchows Arch 431: 425-430, 1997.
50. Wagrowska-Danilewicz M and Danilewicz M: Synaptopodin immunoexpression in steroid-responsive and steroid-resistant minimal change disease and focal segmental glomerulosclerosis. Nefrologia 27: 710-715, 2007.
51. Hu YF, Tan Y, Yu XJ, Wang H, Wang SX, Yu F and Zhao MH: Podocyte involvement in renal thrombotic microangiopathy: A clinicopathological study. Am J Nephrol 51: 752-760, 2020.
52. Kawasaki Y, Imaizumi T, Matsuura H, Ohara S, Takano K, Suyama K, Hashimoto K, Nozawa R, Suzuki H and Hosoya M: Renal expression of alpha-smooth muscle actin and c-Met in children with Henoch-Schönlein purpura nephritis. Pediatr Nephrol 23: 913-919, 2008.
53. Ren X, Guan G, Liu G and Liu G: Irbesartan ameliorates diabetic nephropathy by reducing the expression of connective tissue growth factor and alpha-smooth-muscle actin in the tubulointerstitium of diabetic rats. Pharmacology 83: 80-87, 2009.
54. Hagiwara A, Nishiyama M and Ishizaki S: Branched-chain amino acids prevent insulin-induced hepatic tumor cell proliferation by inducing apoptosis through mTORC1 and mTORC2-dependent mechanisms. J Cell Physiol 227: 2097-2105, 2012.
55. Huo HZ, Zhou ZY, Wang B, Qin J, Liu WY and Gu Y: Dramatic suppression of colorectal cancer cell growth by the dual mTORC1 and mTORC2 inhibitor AZD-2014. Biochem Biophys Res Commun 443: 406-412, 2014.
56. Yang Z, Liu F, Qu H, Wang H, Xiao X and Deng H: 1, 25(OH)2D3 protects β cell against high glucose-induced apoptosis through mTOR suppressing. Mol Cell Endocrinol 414: 111-119, 2015.
57. Cao W, Li M, Wu T, Feng F, Feng T, Xu Y and Sun C: αMSH prevents ROS-induced apoptosis by inhibiting Foxo1/mTORC2 in mice adipose tissue. Oncotarget 8: 40872-40884, 2017.
58. Wang Y, Tao J, Wang M, Yang L, Ning F, Xin H, Xu X, Cai H, Zhang W, Yu K and Zhang X: Mechanism of regulation of big-conductance Ca^{2+}-Activated K^+ Channels by mTOR complex 2 in podocytes. Front Physiol 10: 167, 2019.